Carbon nanotube electrochemical sensor based on and benzofuran derivative as a mediator for the determination of levodopa, acetaminophen, and tryptophan

Mohammad Mazloum-Ardakani · Maryam Zokaie · Alireza Khoshroo

Abstract In this research, a (7,8-dihydroxy-3,3,6-trimethyl-3,4-dihydrodibenzo[b,d]furan-1(2H)-one] (DTDF) multi-walled carbon nanotube modified carbon paste electrode was constructed and used as an excellent electrocatalyst in the oxidation of levodopa (LD) in the presence of acetaminophen (AC) and tryptophan (TRP). In the first part of the work, we synthesized DTDF by electrochemically oxidizing the catechol derivative in the presence of dimedone as a nucleophile in an aqueous solution. A modified carbon paste electrode based on this electrosynthesised compound (DTDF) and carbon nanotubes (CNTs) was prepared. Cyclic voltammetry was used to investigate the redox properties of this modified electrode at various scan rates. Next, the mediated oxidation of LD at the modified electrode was described. At the optimum pH of 7.0, the oxidation of LD occurs at a potential about 330 mV less positive than that of an unmodified carbon paste electrode. Based on differential pulse voltammetry (DPV), the oxidation of LD exhibited a dynamic range between 1.0 and 1000.0 μM and a detection limit of 0.46 μM. DPV was used for simultaneous determination of LD, AC, and TRP at the modified electrode and quantitation of LD, AC, and TRP in some real samples by the standard addition method.

Keywords Electrocatalyst · Levodopa · Electrosynthesis · Carbon nanotubes · Modified electrode

M. Mazloum-Ardakani (✉) · M. Zokaie · A. Khoshroo
Department of Chemistry, Faculty of Science, Yazd University, Yazd 89195-741, Islamic Republic of Iran
e-mail: mazloum@yazd.ac.ir

Introduction

Nanomaterials have received great attention in recent years in different fields due to their enormous potential. Among them, carbon nanotubes (CNTs) have become the subject of intense investigation since their discovery in 1991 by Iijima [1]. Such considerable interest stems from the unique behavior of CNTs, including their remarkable electrical, chemical, mechanical, and structural properties that make them a very attractive material for a wide range of applications [2–4]. The advantages of both single-walled (SW) and multi-walled (MW) CNTs, such as high surface area, good conductance, favorable electronic properties, and electrocatalytic effect, make them adequate for the construction of electrochemical sensor [5, 6].

Carbon paste electrodes (CPEs), due to their ease of construction, renewability, and compatibility with various types of modifiers, have been widely used as a suitable matrix for preparation of modified electrodes. Further, they show a low background current compared to the solid graphite or noble metal electrodes [7]. In recent years, application of the CNT in CPEs showed considerable improvements in electrochemical behavior of biologically important compounds [8–10].

Levodopa (LD) is an important neurotransmitter, which has been used for the treatment of neural disorders such as Parkinson's disease. The cause of Parkinson's disease is the significant depletion of dopamine [11, 12]. After its oral administration, levodopa is absorbed through the bowel and converted to dopamine by decarboxylase. Unfortunately, conversion of levodopa to dopamine in the rest of the body can cause undesirable side effects such as nausea and palpitations. A variety of analytical methods such as spectrophotometry [13], flow injection analysis [14], high-performance liquid chromatography [15], and electroanalysis [16–18] have been developed in order to measure LD levels in different sample matrices.

In contrast, electrochemical methods can offer several advantages, for example, an inexpensive and simple analytical method with remarkable detection sensitivity, reproducibility, and ease of miniaturization [19–25]; they have been used in a wide range of important applications in clinical, industrial, environmental, and agricultural analyses [26–41]

N-Acetyl-p-aminophenol (AC) is a widely used analgesic anti-pyretic drug. It is a suitable alternative for patients who are sensitive to aspirin [42]. However, overdoses of AC can cause liver and kidney damage and possibly mortality [43]. Several techniques such as titrimetry, spectrophotometry, and liquid chromatography [44, 45] have been applied to the determination of AC in pharmaceutical formulations and biological fluids. Titrimetric as well as spectrophotometric methods involve tedious extraction processes prior to the determination, and liquid chromatographic methods are time consuming. Due to the advantages of relatively low cost, fast response, simple instrumentation, high sensitivity, facile miniaturization, and low power requirement, voltammetric methods have been developed for determination of AC [46–48]

Tryptophan (TRP), a vital constituent of proteins and a precursor for biologically important molecules such as the neurotransmitter serotonin and the neurohormone melatonin, is an amino acid essential to humans and animals due to its physiological roles [49]. Also, TRP is a precursor of serotonin (a neurotransmitter), melatonin (a neurohormone), and niacin. It is sometimes added to dietary and feed products as a food fortifier and to pharmaceutical formulations in order to correct possible dietary deficiencies [49]. It is also indispensable in human nutrition for establishing and maintaining a positive nitrogen balance [50]. Unfortunately, TRP cannot be synthesized directly in human body and therefore must be taken from pharmaceutical formulations and TRP-enhanced dietary or food products. Nevertheless, when improperly metabolized, waste products generated in the brain will cause hallucinations and delusions [51]. Given the far reaching role of this amino acid, methods for its detection in food processing, pharmaceutical formulations, and biological fluids are of great importance. Electrochemical methods of detecting TRP [5, 52] have show promise compared to standard chromatographic and electrophoretic methods.

Electrochemistry provides an interesting and versatile means for the study of chemical reactions. The importance of an electrochemical synthesis lies not only in the selectivity of the reaction but also in the formation of electrons at the electrode surface. Hence, since the electrons are reagent free, pollution of the environment by spent reagents can be avoided. In addition, electrosynthesis can lead to efficient and sometimes unexpected synthesis of compounds, which cannot be easily prepared by conventional organic synthesis. The electrochemical generation and study of the intermediates may be advantageous because of the mild reaction conditions

employed and the additional selectivity introduced in controlled potential experiments. For example, catechol and hydroquinone can be easily oxidized to the corresponding reactive o-benzoquinones mainly due to their low oxidation potentials which can be successfully used in the electrosynthesis of many pharmaceutically important compounds [53]. There has been a growing interest in the study of reactions involving quinones produced through the oxidation of catechols versus other nucleophiles. This is due to the mechanistic and synthetic importance of these reactions [54].

According to the above points, it is very important to create suitable conditions for the simultaneous analysis of LD, AC, and TRP in biological samples. However, to the best of our knowledge, there is no report on the voltammetric determination of LD, AC, and TRP simultaneously, using modified carbon nanotube electrodes. Thus, in the present work, we synthesized benzofuran derivatives using the electrosynthesis method. Among the organic compounds, catechols can be easily oxidized to the corresponding reactive o-benzoquinones mainly due to their low oxidation potentials [54]. Therefore, in this work, we describe the preparation of a new electrode composed of carbon nanotube paste electrode (CNPE) modified with 7,8-dihydroxy-3,3,6-trimethyl-3,4-dihydrodibenzo[b,d]furan-1(2H)-one (DTDF) and investigate its performance for the electrocatalytic determination of LD in aqueous solutions. We also evaluate the analytical performance of the modified electrode for quantification of LD in the presence of AC and TRP.

Experimental

Apparatus and chemicals

A potentiostat/galvanostat (SAMA 500, Islamic Republic of Iran) was used for carrying out the electrochemical experiments. A conventional three-electrode cell was used at 25 ± 1 °C. An Ag/AgCl/KCl (3.0 M) reference electrode, a platinum wire auxiliary electrode and a modified carbon paste working electrode. A Metrohm 827 pH/Ion meter was used for pH measurements. All solutions were freshly prepared using double-distilled water. Scanning electron microscopy (SEM) was performed with TESCAN instrument model VEGA3.

LD, AC, TRP, and all other reagents were of analytical grade from Aldrich (USA). Graphite powder and paraffin oil (DC 350, density=0.88 g cm^{-3}) as the binding agent (both from Merck, Germany) were used for preparing the pastes. Multi-walled carbon nanotubes (purity more than 95 %) with 10–20-nm outer diameter, 5–10-nm inner diameters, and 0.5–200-nm tube length were acquired from Nanostructured & Amorphous Materials, Inc. All buffers were prepared from orthophosphoric acid and its salts in the pH range of 2.0–11.0.

Electro-organic synthesis of a catechol derivative

An aqueous sodium acetate solution (80 mL; 0.15 M) containing 2.0 mmol catechol and 2.0 mmol dimedone was electrolyzed in a single-compartment cell equipped with a graphite anode (an assembly of four rods, 6-mm diameter and 6-cm length) and a large platinum gauze cathode at 25 °C under constant current density of 2 mA cm^{-2}. The electrolytic process was interrupted several times to wash the graphite anode in acetone for reactivation. At the end of electrolysis, a few drops of acetic acid were added to the solution and the cell was placed in a refrigerator overnight. The precipitated solid was collected by filtration, washed with water, and then recrystallized from a mixture of water/acetone. The products were characterized by IR, ^{1}H nuclear magnetic resonance (NMR), and ^{13}C NMR [53, 55].

Characteristics of product—7,8-dihydroxy-3,3,6-trimethyl-3,4-dihydrodibenzo[b,d]furan-1(2H)-one ($C_{15}H_{16}O_4$). Applied potential: 0.45 versus SCE. IR (KBr) ν (cm^{-1}): 3496, 3178, 2962, 2925, 1647, 1584, 1527, 1461, 1326, 1302, 1230, 1049, 863, 819, 747. ^{1}H NMR, δ (ppm) (400 MHz, DMSO): 1.01 (s, 3H, methyl), 2.23(s, 3H, methyl), 2.35 (s, 2H, methylene), 2.87 (s, 2H, methylene), 7.07 (s, 1H aromatic); 8.46 (s, 1H hydroxy), 9.38(s, 1H hydroxy). ^{13}C NMR, δ (ppm) (DMSO): 9.43, 28.50, 35.40, 37.25, 51.97, 102.76, 108.38, 113.77, 115.09, 142.48, 143.76, 148.41, 168.92, 194.26.

Preparation of the electrode

The DTDF–CNPEs were prepared by hand mixing 0.005 g of DTDF with 0.5 g graphite powder and 0.015 g CNTs with a mortar and pestle. Then, 0.7 mL of paraffin was added to the above mixture and mixed for 20 min until a uniformly wetted paste was obtained. The paste was then packed into the end of a glass tube (ca. 3.4 mm i.d. and 10 cm long). A copper wire inserted in the carbon paste provided electrical contact. When necessary, a new surface was obtained by pushing an excess of the paste out of the tube and polishing with a weighing paper. For comparison, DTDF modified CPE (DTDF–CPE) without CNTs, CNT paste electrode (CNPE) without DTDF, and unmodified CPE in the absence of both DTDF and CNTs were also prepared in the same way.

Results and discussion

Scanning electron microscopic characterization

Typical SEM images of different electrodes were shown in Fig. 1. Figure 1a shows the layer of graphite powder and isolated with each other on the surface of CPE. After CNTs added to the carbon paste, it can be seen that CNTs were distributed on the paste with special three-dimensional structure, indicating that the CNTs were successfully modified on the CNPE (Fig. 1b).

Electrochemical properties of modified DTDF–CNPE

To the best of our knowledge, there is no prior report on the electrochemical properties and, in particular, the electrocatalytic activity of DTDF in aqueous media. Therefore, we prepared modified electrodes based on DTDF–CNPE and studied their electrochemical properties in a pH 7.0 phosphate buffer using cyclic voltammetry (CV). The cyclic voltammogram obtained at a DTDF–CNPE in a pH 7.0 phosphate buffer is shown in Fig. 2. This figure displays reproducible, well-
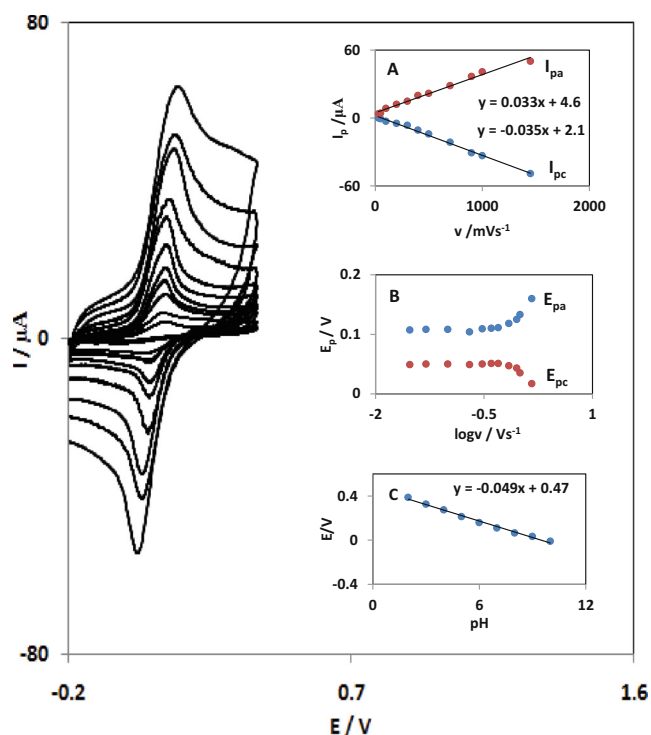

Fig. 1 SEM images of a CPE and b DTDF–CNPE
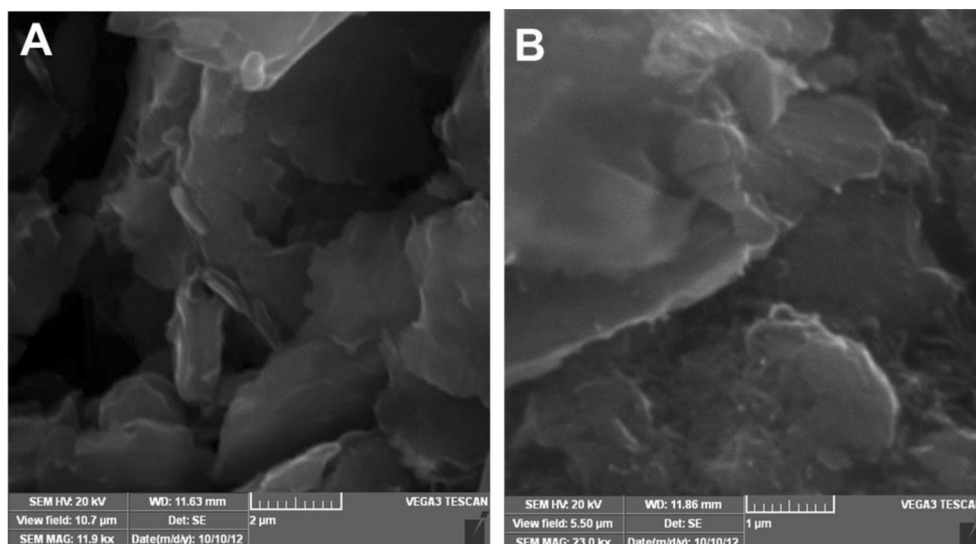
Fig. 2 Cyclic voltammograms of DTDF–CNPE in 0.1 M phosphate-buffered solution (pH 7.0) at different scan rates, from down to up: 30, 50, 100, 200, 300, 500, 700, 900, 1000, 1300, and 1450 mV s^{-1}; insets: **a** variation of I_p versus scan rate; **b** E_p versus the logarithm of scan rates

defined anodic peak arising from the oxidation of DTDF to its quinone with E_{pa} at 0.113 V and cathodic peak arising from the reduction of the quinone back to DTDF with E_{pc} at 0.055 V versus Ag|AgCl|KCl (3.0 M). The observed peak potential separation, $\Delta E_p = (E_{pa} - E_{pc})$ of 168 mV, was greater than the value of 59/n mV expected for a reversible system, suggesting that the redox couple of DTDF in DTDF–CNPE has a quasi-reversible behavior in aqueous medium [56]. The effect of the potential scan rate (υ) on electrochemical properties of the DTDF–CNPE was also studied by CV. Plots of both anodic and cathodic peak currents (I_p) were linearly dependent on υ in the range of 100–1500 mV s^{-1} (Fig. 2a), indicating that the redox process of DTDF at the modified electrode is diffusionless in nature [56].

The apparent charge transfer rate constant, k_s, and the charge transfer coefficient, α, of a surface-confined redox couple can be evaluated from CV experiments using the variation of anodic and cathodic peak potentials with logarithm of scan rate, according to the procedure reported by Laviron [57]. Based on the equation, the cathodic transfer coefficient, α_c, and the anodic transfer coefficient, α_a, can be estimated from the slope of an E_{pc} versus log ν, $-2.303RT/\alpha nF$, and the slope of an E_{pa} versus log ν, 2.303 RT/$(1-\alpha)nF$. Accordingly, α_c and α_a were both estimated to be 0.5. Next,

based on Eq. (1), k_s between the modifying agent, DTDF and CNPE can be evaluated:

$$\log k_s = \alpha \log(1-\alpha)$$
$$+ (1-\alpha) \log \alpha - \log\left(\frac{RT}{nFT\vartheta}\right) - \alpha(1-\alpha)\frac{nF\Delta E_p}{2.3RT} \quad (1)$$

where $(1-\alpha) = 0.5$ and all other symbols having their conventional meanings. The average value of k_s for five CVs was evaluated to be 4.8 ± 0.3 s^{-1} using Eq. (1).

Influence of pH

The electrochemistry of DTDF molecule is generally pH dependent. Thus, the electrochemical behavior of DTDF–CNPE was studied at different pHs using CV. It was observed that the anodic and cathodic peak potentials of DTDF–CNPE shift to less positive values with increasing pH. Figure 2c shows potential-pH diagrams constructed by plotting the half-wave potential (estimated by the average of both anodic and cathodic peak potential) as the function of pH. It is clearly seen that all the one plots are straight lines with slopes near 49.0 mV/pH, indicating that the system obeys the Nernst equation for a two-electron and two-proton transfer reaction [56].

Electrocatalytic oxidation of LD at a DTDF–CNPE

Figure 3 depicts the CVs for unmodified CPE in buffer (curve a) and electrochemical oxidation of 0.3 mM LD at unmodified CPE (curve b), CNPE (curve d), DTDF–CPE (curve e), and DTDF–CNPE (curve f). As it is seen, at the unmodified CPE and without the mediator, no peak is observed in the buffer solution (curve a), while the anodic peak potential for LD oxidation at the CNPE and unmodified CPE are 580 and 610 mV, respectively, the corresponding peak potential at DTDF–CNPE is 185 mV, corresponding to a negative shift of approximately 425 mV compared to those obtained at the two former electrodes. However, DTDF–CNPE show a 45 % higher anodic peak current for the oxidation of LD compared to DTDF–CPE, indicating that the combination of CNTs and the mediator (DTDF) has significantly improved the performance of the electrode toward LD oxidation. In fact, DTDF–CNPE in the absence of LD exhibited a well-behaved redox reaction (Fig. 3, curve c) in 0.1 M phosphate buffer (pH 7.0), which anodic peak arising from the oxidation of DTDF to its quinone and cathodic peak arising from the reduction of the quinone back to DTDF. However, there was a drastic increase in the anodic peak current in the presence of 0.3 mM LD (curve f), which can be related to the strong electrocatalytic effect of the DTDF–CNPE toward this compound.
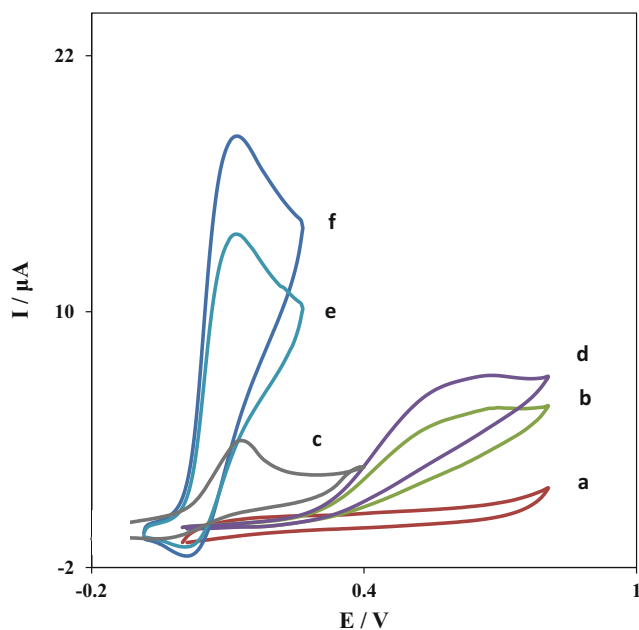
Fig. 3 CVs of **a** unmodified CPE in 0.1 M phosphate-buffered solution (pH 7.0) at scan rate of 30 mV s^{-1}; **b** as **a**+0.3 mM LD; **c** as **a** at the surface of DTDF–CNPE; **d** as **b** at the surface of CNPE; **e** as **b** at the surface of DTDF–CPE; **f** as **b** at the surface of DTDF–CNPE
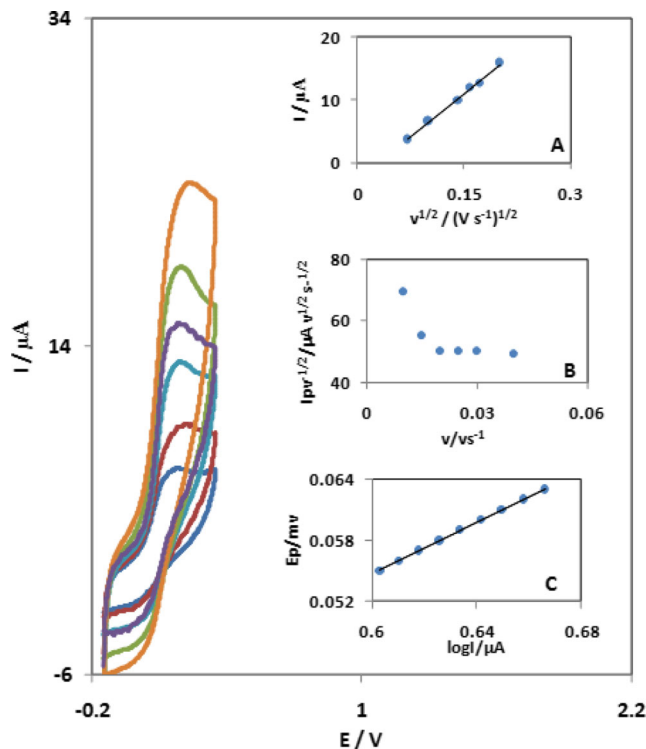

Fig. 4 CVs of DTDF–CNPE in 0.1 M phosphate-buffered solution (pH 7.0) containing 0.3 mM LD at various scan rates, from inner to outer scan rates of 5, 10, 20, 25, 30, and 40 mV s^{-1}, respectively. Insets: variation of **a** anodic peak current versus $\upsilon^{1/2}$; **b** normalized current ($I_p/\upsilon^{1/2}$) versus υ; **c** Tafel plot derived from the rising part of voltammogram recorded at a scan rate of 10 mV s^{-1}

The effect of scan rate on the electrocatalytic oxidation of LD at the DTDF–CNPE was investigated by CV (Fig. 4). The plot of peak height (I_p) versus the square root of scan rate ($\upsilon^{1/2}$), in the range of 5–40 mV s^{-1} is shown in Fig. 4 (inset A). This plot was found to be linear, suggesting that at sufficient overpotential, the process was diffusion rather than surface controlled. A plot of the sweep rate normalized current ($I_p/\upsilon^{1/2}$) versus sweep rate (Fig. 4, inset B) exhibits the characteristic shape typical of an EC′ process [56]. In this mechanism, LD is oxidized in the catalytic chemical reaction (C′) by the oxidized form of DTDF (DTDF$_{ox}$) which produced via an electrochemical reaction (E). Therefore, when the DTDF is oxidized at the potential of 185 mV, the LD can be oxidized too in this potential. Thus, the LD is oxidized at the potential of 185 mV at the DTDF–CNPE while it is oxidized at 610 mV at the bare electrode.

The inset C of Fig. 4 shows the Tafel plot for the sharp rising part of the voltammogram. If deprotonation of LD is a sufficiently fast step, the Tafel plot can be used to estimate the number of electrons involved in the rate-determining step. A Tafel slope of 0.126 V decade^{-1} was obtained which agrees well with the involvement of one electron in the rate determining step of the electrode process, assuming a transfer coefficient, α, of 0.53.

Chronoamperometric measurements

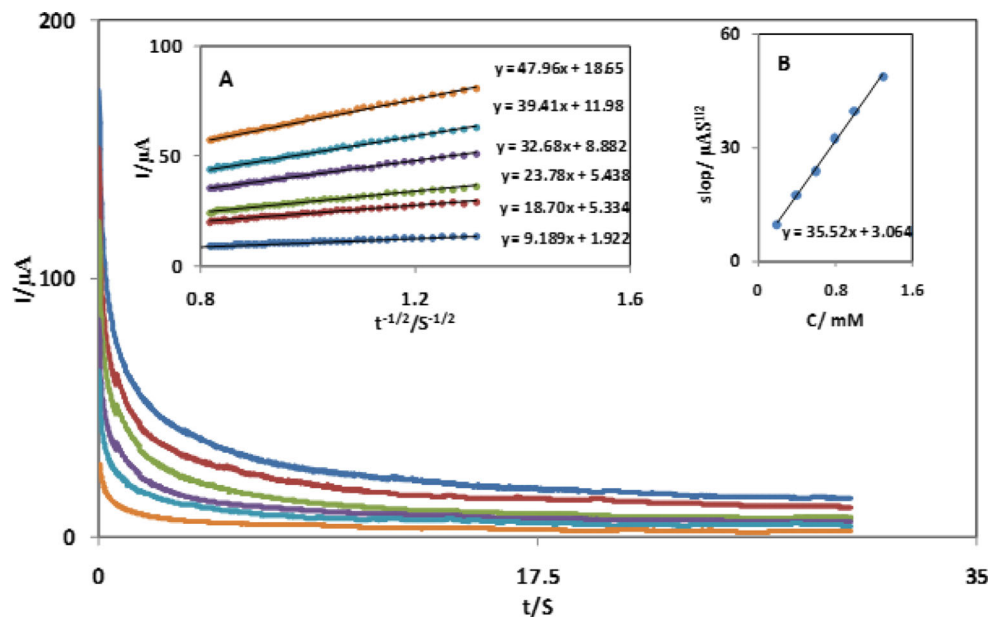Chronoamperometric measurements of LD at DTDF–CNPE were carried out at the working electrode potential of 300 mV

for various concentrations of LD (Fig. 5). For an electroactive material (LD in this case) with a diffusion coefficient of D, the current observed for the electrochemical reaction at the mass transport limited conditions can be described by the Cottrell equation [56]. Experimental I versus $t^{-1/2}$ plots were constructed, with the best fits for different concentrations of LD. The slopes of the resulting straight lines were then plotted versus LD concentration. From the resulting slope and Cottrell equation, the mean value of the D was found to be 1.03×10^{-5} cm^2 s^{-1}.

Chronoamperometry can also be employed to evaluate the catalytic rate constant, k, for the reaction between LD and the DTDF–CNPE according to the method of Galus [58]:

$$\frac{I_C}{I_L} = \gamma^{1/2}\left[\pi^{1/2}\mathrm{erf}\left(\gamma^{\S}\right) + \frac{\exp(-\gamma)}{\gamma^{1/2}}\right] \quad (2)$$

where I_C is the catalytic current of LD at the DTDF–CNPE, I_L is the limited current in the absence of LD, and $\gamma = kC_bt$ is the argument of the error function (C_b is the bulk concentration of LD). In cases where γ exceeds the value of 2, the error

function is almost equal to 1 and therefore, the above equation
can be reduced to

$$\frac{I_C}{I_L} = \pi^{1/2}\gamma^{1/2} = \pi^{1/2}(kC_bt)^{1/2} \qquad (3)$$

where t is the time elapsed. The above equation can be used to
calculate the rate constant, k, of the catalytic process from the
slope of I_C/I_L versus $t^{1/2}$ at a given LD concentration. From the
values of the slopes, the average value of k was found to be
2.7×10^4 M^{-1} s^{-1}.

Calibration plot and detection limit

DPV was used to obtain the linear concentration range and
detection limit of LD at the DTDF–CNPE (Fig. 6). The plot of
peak current versus LD concentration consisted of two linear
segments with slopes of 0.110 and 0.033 μA μM^{-1} in the
concentration ranges of 1.0–80.0 and 80.0–1000.0 μM, re-
spectively. The decrease in sensitivity (slope) of the second
linear segment is likely due to kinetic limitation. The detection
limit (3σ) was calculated from the first linear segment of the
calibration plot as 0.46 μM.

Interference study

The influence of various foreign species on the determination
of 1.0×10^{-4} M LD was investigated. The tolerance limit was
taken as the maximum concentration of the foreign sub-
stances, which caused an approximately ±5 % relative error
in the determination. The tolerated concentration of foreign
substances was 1.0×10^{-1} M for Cl$^-$, Na$^+$, NO$_3^-$, F$^-$, S^{2-},

CO$_3^{2-}$, HCO$_3^-$, and K$^+$; 5.0×10^{-2} M for Mg^{2+}, Ba^{2+}, Cd^{2+},
Cu^{2+}, Pb^{2+}, Ni^{2+}, Al^{3+}, and Ca^{2+}; and 5.0×10^{-3} M for glu-
cose, lactose, fructose, sucrose, L-cysteine, L-asparagines, L-
glycine, L-glutamic acid, D-penicillamine, folic acid, uric acid,
and guanine. However, equal molars of methyl dopa, ascorbic
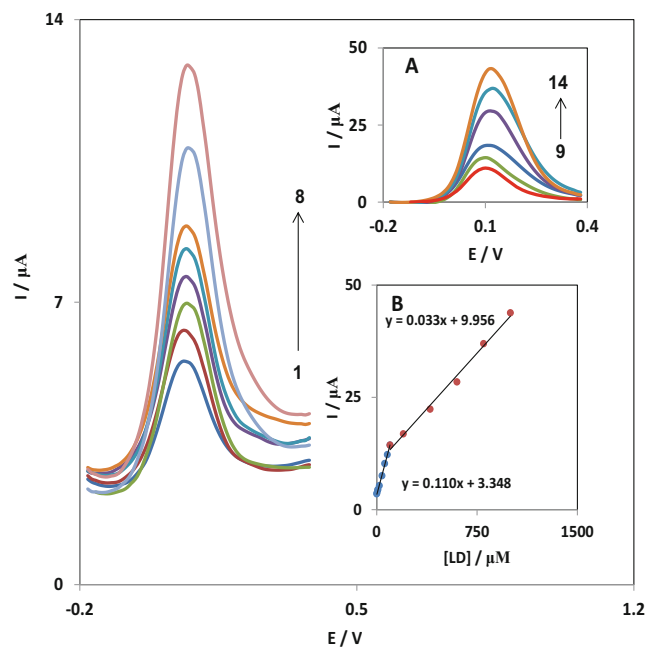acid, and carbidopa cause serious interference.



Fig. 6 Differential pulse voltammograms of DTDF–CNPE in
0.1 M phosphate-buffered solution (pH 7.0) containing different
concentrations of LD. The numbers 1–14 correspond to 1.0, 3.0,
8.0, 10.0, 20.0, 40.0, 60.0, 80.0, 100.0, 200.0, 400.0, 600.0, 800.0,
and 1000.0 μM of DA. Inset B shows the plots of the peak current
as a function of LD concentration in the range of 1.0–80.0 and
80.0–1000.0 μM

Fig. 7 DPVs of DTDF–CNPE in 0.1 M phosphate-buffered solution (pH 7.0) containing different concentrations of LD+AC+TRP (in μM), from inner to outer: 200.0+124.0+100.0, 300.0+187.0+150.0, 400.0+249.0+200.0, 500.0+312.0+250.0, 600.0+375.0+300.0, and 800.0+500.0+400.0, respectively
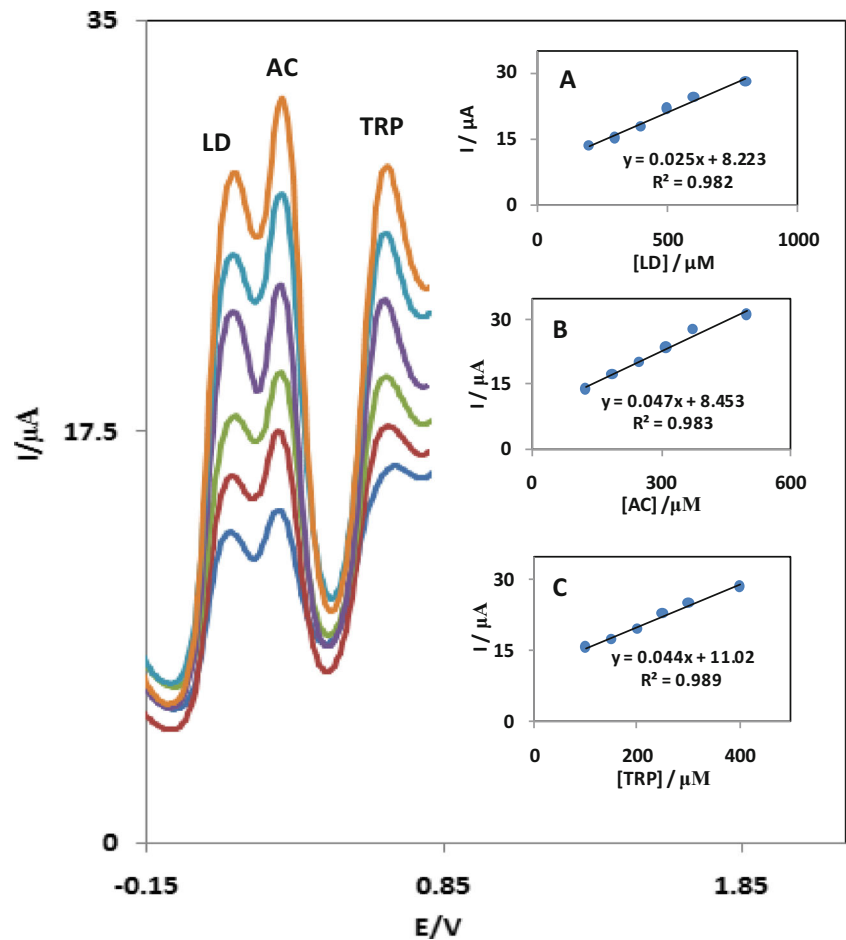
Determination of LD in the presence of AC and TRP

The main objective of this study is to detect LD in the presence of AC and TRP. The utilization of the DTDF–CNPE for the simultaneous determination of LD, AC, and TRP was demonstrated by simultaneously changing the concentrations of LD, AC, and TRP. The DPV results show that the simultaneous determination of LD, AC, and TRP with three well-distinguished anodic peaks at 120, 300, and 630 mV (by DPV technique), corresponding to the oxidation LD, AC, and TRP, respectively, could be possible at the DTDF–CNPE (Fig. 7).

Also, using DTDF–CNPE as the working electrode, we obtained the linear range simulation of the calibration curve for AC and TRP as 100.0–500.0 and 100.0–400.0 μM, respectively, and the detection limit 1.11 and 1.16 μM respectively.

Real-life sample analysis

The proposed electrocatalytic sensor was used to determine LD, AC, and TRP in human blood serum samples. The samples were found to be free from LD, AC, and TRP. Therefore, different amounts of LD, AC, and TRP were spiked to the sample and analyzed by the proposed method. The results for determination of the three species in blood serum samples are given in Table 1, showing the average

Table 1 The application of DTDF–CNPE for simultaneous determination of LD, AC, and TRP in human blood serum sample ($n=4$)

NA	LD added (μM)	LD found (μM)	Recovery (%)	RSD (%)	AC added (μM)	AC found (μM)	Recovery (%)	RSD (%)	TRP added (μM)	TRP found (μM)	Recovery (%)	RSD (%)
1	0	ND	–	–	0	ND	–	–	0	ND	–	–
2	400	380.7	95.1	2.7	249	262.5	105.4	3.1	200	191.7	95.8	2.6
3	600	582.0	97.0	1.9	375	394.0	105.3	2.3	300	302.99	100.9	3.2
4	800	796.0	99.5	2.4	500	522.2	104.0	2.6	400	420.7	105.1	2.7

recovery percent and the residual standard deviation (RSD) for LD contents. These results show the capability of the DTDF–CNPE in determination of LD in human blood serum samples with good reproducibility.

Conclusions

In the present study, DTDF–CNPEs were used in the determination of LD in the presence of AC and TRP. The CV and DPV investigations showed effective electrocatalytic activity of the modified electrode in lowering the anodic overpotential for the oxidation of LD. The detected potential differences of 180, 510, and 330 mV between LD–AC, LD–TRP, and AC–TRP, respectively, are large enough to allow simultaneous determinationof LD, AC, and TRP in mixtures without significant interferences. High sensitivity, selectivity, and reproducibility of the voltammetric responses and detection limit (0.46 μM), together with the ease of preparation and surface regeneration, makes the proposed modified electrode very useful for accurate determination of LD in real-life samples.

References

1. Iijima S, Ichihashi T (1993) Single-shell carbon nanotubes of 1-nm diameter. Nature 363:603–605
2. Mazloum-Ardakani M, Sheikh-Mohseni MA (2011) Carbon Nanotubes in Electrochemical Sensors, Carbon Nanotubes - Growth and Applications, Dr. Mohammad Naraghi (Ed.), InTech, doi:10.5772/20604
3. Mazloum-Ardakani M, Khoshroo A (2014) Electrocatalytic properties of functionalized carbon nanotubes with titanium dioxide and benzofuran derivative/ionic liquid for simultaneous determination of isoproterenol and serotonin. Electrochim Acta 130:634–641
4. Goyal RN, Gupta VK, Chatterjee S (2008) Simultaneous determination of adenosine and inosine using single-wall carbon nanotubes modified pyrolytic graphite electrode. Talanta 76:662–668
5. Mazloum-Ardakani M, Sabaghian F, Khoshroo A et al (2014) Electrochemical determination of captopril in the presence of acetaminophen, tryptophan, folic acid, and l-cysteine at the surface of modified carbon nanotube paste electrode. Ionics 25:1–12
6. Luo S, Wu Y, Gou H (2013) A voltammetric sensor based on GO–MWNTs hybrid nanomaterial-modified electrode for determination of carbendazim in soil and water samples. Ionics 19:673–680
7. Adams R (1958) Carbon paste electrodes. Anal Chem 30:1576
8. Mazloum-Ardakani M, Ahmadi SH, Mahmoudabadi ZS, et al. (2014) Electrochemical and catalytic investigations of epinephrine, acetaminophen and folic acid at the surface of titanium dioxide nanoparticle-modified carbon paste electrode. Ionics 20:1757–1765
9. Mazloum-Ardakani M, Sheikh-Mohseni M, Mirjalili B-F (2014) Nanomolar detection limit for determination of norepinephrine in the presence of acetaminophen and tryptophan using carbon nanotube-based electrochemical sensor. Ionics 20:431–437
10. Ensafi AA, Izadi M, Karimi-Maleh H (2013) Sensitive voltammetric determination of diclofenac using room-temperature ionic liquid-modified carbon nanotubes paste electrode. Ionics 19:137–144
11. Hardy J, Gwinn-Hardy K (1998) Genetic classification of primary neurodegenerative disease. Science 282:1075–1079
12. Katzenschlager R, Poewe W (2014) Parkinson disease: intestinal levodopa infusion in PD—the first randomized trial. Nat Rev Neurol 10:128–129
13. Nagaraja P, Murthy KC, Rangappa KS, Gowda NM (1998) Spectrophotometric methods for the determination of certain catecholamine derivatives in pharmaceutical preparations. Talanta 46: 39–44
14. Fatibello-Filho O, da Cruz Vieira I (1997) Flow injection spectrophotometric determination of L-dopa and carbidopa in pharmaceutical formulations using a crude extract of sweet potato root [*Ipomoea batatas* (L.) Lam.] as enzymatic source. Analyst (Cambridge, U K) 122:345–350
15. Doležalová M, Tkaczykova M (1999) Direct high-performance liquid chromatographic determination of the enantiomeric purity of levodopa and methyldopa: comparison with pharmacopoeial polarimetric methods. J Pharm Biomed Anal 19:555–567
16. Mazloum-Ardakani M, Khoshroo A (2013) Nano composite system based on coumarin derivative–titanium dioxide nanoparticles and ionic liquid: Determination of levodopa and carbidopa in human serum and pharmaceutical formulations. Anal Chim Acta 798:25–32
17. Mazloum-Ardakani M, Taleat Z, Khoshroo A et al (2012) Electrocatalytic oxidation and voltammetric determination of levodopa in the presence of carbidopa at the surface of a nanostructure based electrochemical sensor. Biosens Bioelectron 35:75–81
18. Mazloum-Ardakani M, Sheikh-Mohseni MA, Abdollahi-Alibeik M, Benvidi A (2012) Application of nanosized MCM-41 to fabrication of a nanostructured electrochemical sensor for the simultaneous determination of levodopa and carbidopa. Analyst (Cambridge, U K) 137:1950–1955
19. Goyal RN, Gupta VK, Chatterjee S (2008) Electrochemical oxidation of 2′,3′-dideoxyadenosine at pyrolytic graphite electrode. Electrochim Acta 53:5354–5360
20. Goyal RN, Gupta VK, Bachheti N, Sharma RA (2008) Electrochemical sensor for the determination of dopamine in presence of high concentration of ascorbic acid using a Fullerene-C60 coated gold electrode. Electroanalysis 20:757–764
21. Gupta VK, Mangla R, Khurana U, Kumar P (1999) Determination of uranyl ions using poly(vinyl chloride) based 4-tert-butylcalix [6]arene membrane sensor. Electroanalysis 11:573–576
22. Gupta VK, Prasad R, Kumar P, Mangla R (2000) New nickel (II) selective potentiometric sensor based on 5, 7, 12, 14-tetramethyldibenzotetraazaannulene in a poly (vinyl chloride) matrix. Anal Chim Acta 420:19–27
23. Gupta VK, Prasad R, Kumar A (2003) Preparation of ethambutol–copper (II) complex and fabrication of PVC based membrane potentiometric sensor for copper. Talanta 60:149–160
24. Gupta VK, Nayak A, Agarwal S, Singhal B (2011) Recent advances on potentiometric membrane sensors for pharmaceutical analysis. Comb Chem High Throughput Screen 14:284–302
25. Jain AK, Gupta VK, Singh LP, Raisoni JR (2006) A comparative study of Pb2+ selective sensors based on derivatized tetrapyrazole and calix [4] arene receptors. Electrochim Acta 51:2547–2553, 18
26. Gupta VK, Jain S, Khurana U (1997) A PVC-based pentathia-15-crown-5 membrane potentiometric sensor for mercury(II). Electroanalysis 9:478–480
27. Gupta VK, Sethi B, Sharma RA et al (2013) Mercury selective potentiometric sensor based on low rim functionalized thiacalix [4]-arene as a cationic receptor. J Mol Liq 177:114–118

28. Gupta VK, Chandra S, Mangla R (2002) Dicyclohexano-18-crown-6 as active material in PVC matrix membrane for the fabrication of cadmium selective potentiometric sensor. Electrochim Acta 47: 1579–1586

29. Gupta VK, Jain S, Chandra S (2003) Chemical sensor for lanthanum(III) determination using aza-crown as ionophore in poly(-vinyl chloride) matrix. Anal Chim Acta 486:199–207

30. Gupta VK, Chandra S, Lang H (2005) A highly selective mercury electrode based on a diamine donor ligand. Talanta 66:575–580

31. Gupta VK, Jain AK, Maheshwari G et al (2006) Copper (II)-selective potentiometric sensors based on porphyrins in PVC matrix. Sensor Actuator B Chem 117:99–106

32. Gupta VK, Singh AK, Mehtab S, Gupta B (2006) A cobalt(II)-selective PVC membrane based on a Schiff base complex of N, N′-bis(salicylidene)-3,4-diaminotoluene. Anal Chim Acta 566:5–10

33. Prasad R, Gupta VK, Kumar A (2004) Metallo-tetraazaporphyrin based anion sensors: regulation of sensor characteristics through central metal ion coordination. Anal Chim Acta 508:61–70

34. Gupta VK, Jain AK, Kumar P (2006) PVC-based membranes of N, N′-dibenzyl-1, 4, 10, 13-tetraoxa-7, 16-diazacyclooctadecane as Pb (II)-selective sensor. Sensor Actuator B Chem 120:259–265

35. Gupta VK, Jain AK, Kumar P et al (2006) Chromium(III)-selective sensor based on tri-o-thymotide in PVC matrix. Sensor Actuator B Chem 113:182–186

36. Gupta VK, Singh AK, Al Khayat M, Gupta B (2007) Neutral carriers based polymeric membrane electrodes for selective determination of mercury (II). Anal Chim Acta 590:81–90

37. Gupta VK, Singh LP, Singh R et al (2012) A novel copper (II) selective sensor based on dimethyl 4, 4′(o-phenylene) bis (3-thioallophanate) in PVC matrix. J Mol Liq 174:11–16

38. Srivastava SK, Gupta VK, Jain S (1996) PVC-based 2, 2, 2-cryptand sensor for zinc ions. Anal Chem 68:1272–1275

39. Jain A, Gupta V, Singh L, others (1997) Macrocycle based membrane sensors for the determination of cobalt(II) ions. Analyst 122:583–586

40. Gupta VK, Ganjali MR, Norouzi P et al (2011) Electrochemical analysis of some toxic metals by ion–selective electrodes. Crit Rev Anal Chem 41:282–313

41. Goyal RN, Gupta VK, Bachheti N (2007) Fullerene-C60-modified electrode as a sensitive voltammetric sensor for detection of nandrolone—an anabolic steroid used in doping. Anal Chim Acta 597:82–89

42. Ford MD (2001) Clinical toxicology. Saunders, Philadelphia, PA

43. Smilkstein MJ, Knapp GL, Kulig KW, Rumack BH (1988) Efficacy of oral N-acetylcysteine in the treatment of acetaminophen overdose. N Engl J Med 319:1557–1562

44. Bosch ME, Sanchez AJ, Rojas FS, Ojeda CB (2006) Determination of paracetamol: historical evolution. J Pharm Biomed Anal 42:291–321

45. Roggo Y, Chalus P, Maurer L et al (2007) A review of near infrared spectroscopy and chemometrics in pharmaceutical technologies. J Pharm Biomed Anal 44:683–700

46. Mazloum-Ardakani M, Hosseinzadeh L, Khoshroo A et al (2014) Simultaneous determination of isoproterenol, acetaminophen and folic acid using a novel nanostructure-based electrochemical sensor. Electroanalysis 26:275–284

47. Mazloum-Ardakani M, Sheikh-Mohseni MA, Mirjalili B-F, Zamani L (2012) Simultaneous determination of captopril, acetaminophen and tryptophan at a modified electrode based on carbon nanotubes. J Electroanal Chem 686:12–18

48. Gupta VK, Jain R, Radhapyari K et al (2011) Voltammetric techniques for the assay of pharmaceuticals—a review. Anal Biochem 408:179–196

49. Wurtman RJ, Hefti F, Melamed E (1980) Precursor control of neurotransmitter synthesis. Pharmacol Rev 32:315–335

50. Munn DH, Zhou M, Attwood JT et al (1998) Prevention of allogeneic fetal rejection by tryptophan catabolism. Science 281:1191–1193

51. Grahame Smith DG (1971) Inhibitory effect of chlorpromazine on the syndrome of hyperactivity produced by l-tryptophan or 5-methoxyN, dimethyltryptamine in rats treated with a monoamine oxidase inhibitor. Br J Pharmacol 43:856–864

52. Fouladgar M, Karimi-Maleh H, Hosseinzadeh R (2013) Novel nanostructured electrochemical sensor for voltammetric determination of N-acetylcysteine in the presence of high concentrations of tryptophan. Ionics 19:665–672

53. Nematollahi D, Habibi D, Rahmati M, Rafiee M (2004) A facile electrochemical method for synthesis of new benzofuran derivatives. J Org Chem 69:2637–2640, 20

54. Nematollahi D, Rafiee M, Fotouhi L (2009) Mechanistic study of homogeneous reactions coupled with electrochemical oxidation of catechols. J Iran Chem Soc 6:448–476

55. Mazloum-Ardakani M, Khoshroo A, Nematollahi D, Mirjalili B-F (2012) Electrochemical study of catechol derivatives in the presence of β-diketones: synthesis of benzofuran derivatives. J Electrochem Soc 159:H912–H917

56. Bard AJ, Faulkner LR (2000) Electrochemical methods: fundamentals and applications, 2nd ed. Wiley, New York, p 237, 33, 497, 163

57. Laviron E (1979) General expression of the linear potential sweep voltammogram in the case of diffusionless electrochemical systems. J Electroanal Chem Interfacial Electrochem 101: 19–28

58. Galus Z, Reynolds GF, Marcinkiewicz S (1976) Fundamentals of electrochemical analysis. Ellis Horwood, New York